Smart Forestry

ORIGINAL RESEARCH

Open Access

https://doi.org/10.48130/smartfor-0026-0008

Smart Forestry **2026**, 1: e012

An integrated approach for estimating forest attributes by combining handheld mobile laser scanning with forest models in dense canopy environments

Ziyan Zhang[1], Xiaozi Zhou[1], Zimeng Li[1], Zhaolong Li[1], Zeyu Yang[1], Zhiqiang Guo[1], Lei Hu[2], Lingya Huang[1] and Yuanyong Dian[1,3,4*]

[1] *College of Horticulture and Forestry Sciences, Huazhong Agricultural University, Wuhan, Hubei 430070, China*
[2] *The Forestry Prospect & Design Institute Of Hubei Province, Wuhan, Hubei 430070, China*
[3] *Hubei Engineering Technology Research Centre for Forestry Information, Huazhong Agricultural University, Wuhan, Hubei 430070, China*
[4] *Key laboratory of urban agriculture in central China, Ministry of Agriculture, Wuhan, Hubei 430070, China*
* Correspondence: dianyuanyong@mail.hzau.edu.cn (Dian Y)

Abstract

Accurate estimation of forest attributes is essential for sustainable forest management. While handheld mobile laser scanning (HMLS) enables efficient data collection, its application in complex terrain with dense canopies remains challenging. This study developed an integrated method combining forest models with HMLS data to estimate key forest attributes. The approach involves two steps: (1) reconstructing stem curves from multi-height diameters, and (2) applying stand-level height-diameter (H-D) models to estimate heights for unreconstructed trees. The method was validated using 12 plots in the Shennongjia Forest area encompassing diverse forest characteristics. Results showed that the bias, relative bias (rbias), mean absolute error (MAE), relative MAE (rMAE), root mean square error (RMSE), and relative RMSE (rRMSE) for diameter at breast height (DBH) were 0.3 cm, 1.28%, 0.7 cm, 3.57%, 1.5 cm, and 7.32%, respectively. For tree height, the bias, rbias, MAE, rMAE, RMSE, and rRMSE were −0.3 m, −2.11%, 1.5 m, 11.21%, 2.4 m, and 17.55%, respectively. Stem volume showed a bias, rbias, MAE, rMAE, RMSE, and rRMSE of −0.0012 m^3, −0.32%, 0.0417 m^3, 11.27%, 0.0886 m^3, and 23.92%, respectively. The stand volume exhibited a bias, rbias, MAE, rMAE, RMSE and rRMSE of −1.52 m^3/ha, −0.63%, 10.10 m^3/ha, 4.20%, 12.49 m^3/ha, and 5.19%, respectively. Overall, DBH was slightly overestimated, height was underestimated, and volume accuracy varied by forest type, with plantations demonstrating higher accuracy than natural forests. This approach demonstrates the potential of integrating HMLS with modeling techniques to reliably estimate forest attributes even under dense canopy conditions.

Keywords: Handheld Mobile Laser Scanning, Forest attributes, Dense canopy, Stem curve model, Tree height, Volume

Citation: Zhang Z, Zhou X, Li Z, Li Z, Yang Z, et al. 2026. An integrated approach for estimating forest attributes by combining handheld mobile laser scanning with forest models in dense canopy environments. *Smart Forestry* 1: e012 https://doi.org/10.48130/smartfor-0026-0008

Introduction

Forests, as the largest terrestrial ecosystem, provide various ecosystem services, including carbon sequestration, climate mitigation, biodiversity conservation, and the provision of timber resources[1–3]. Timely and accurate monitoring of forest status and changes is critical for effective forest management and the design of conservation policies[4,5]. Forest inventories, which are essential for obtaining key forest parameters such as diameter at breast height (DBH), tree height, and volume, play a vital role in forest management.

Conventional forest surveying methods, which primarily involve manual, on-site measurements using diameter tapes and altimeters, are not only costly and time-consuming, but also prone to large errors in complex terrain and stand conditions[6]. To address these drawbacks, recent advancements have seen the adoption of technologies such as Light Detection and Ranging (LiDAR). LiDAR, in particular, stands out for its ability to penetrate forest canopies, offering a significant edge in lower-cost and accurate forest surveying[7–10].

LiDAR systems on ground platforms are increasingly used for investigating forest attributes. These systems are commonly classified as ground-based LiDAR systems, such as Terrestrial Laser Scanning (TLS), and mobile LiDAR systems (MLS). TLS can accurately capture three-dimensional forest structure point cloud data[11], widely applied in forest inventories to extract parameters like DBH, tree height, and volume in plantations and urban parks (RMSE = 0.7–4.2 cm)[12,13]. The reconstruction of stem taper curves using TLS has become a critical approach for structural parameters estimation. Recent studies have demonstrated that individual tree stem curve reconstruction and volume estimation can be effectively conducted using backpack LiDAR systems[14]. Under the condition of complete structural coverage of the stem, the combination of model fitting and point cloud density optimization has yielded high accuracy, with rRMSE values below 10%[14,15]. However, single-site TLS may face occlusion issues, resulting in incomplete tree trunk point cloud data. Consequently, multiple-site scanning is often required to obtain a comprehensive forest point cloud[16–18]. Nevertheless, this approach can reduce the efficiency and portability of TLS[19].

MLS offers a larger scanning range and increased flexibility, enabling operators to collect data with reduced understory occlusion and improved efficiency[20]. However, the backpack-type systems face limitations like heavier equipment and operational challenges in complex, steep forest plots. Additionally, in extremely complex environments, point cloud reconstruction may encounter difficulties, requiring the combined use of Simultaneous Localization and Mapping (SLAM), and Global Navigation Satellite Systems (GNSS), to successfully reconstruct dense point clouds[21]. SLAM-based reconstruction algorithms may struggle in extremely intricate environments. In contrast, handheld portable LiDAR is lighter and

more portable, adapting better to diverse terrains and complex forest settings. Both mobile LiDAR systems have been successful in measuring DBH and stand volume. Studies indicate that handheld mobile laser scanning (HMLS) performs well in estimating DBH, but it cannot accurately scan the canopy top, thus hindering precise tree height estimation and subsequently affecting timber volume calculations[22,23]. Moreover, one of the challenges in using HMLS is the presence of understory vegetation, which can partially obstruct the scanning of the lower trunk section. Although HMLS provides high-resolution point clouds near the ground, dense or tall understory vegetation may obscure parts of the trunk, reducing the completeness of stem point clouds. This incomplete coverage can affect the accuracy of stem taper reconstruction and subsequently influence tree height estimation based on model fitting[24,25].

The main challenge of HMLS is its limited scanning range, which can be shorter than tree height[26]. This limitation restricts their effectiveness in capturing complete canopy trunk data in complex forest stand conditions, resulting in underestimation of tree height[14,26]. In this study, 'complex forest stands' and 'dense canopy environments' refer to forest structures characterized by high stem density, multi-layered canopies, and significant understory vegetation. These structural factors, particularly in the upper sections of trees, lead to imbalances or deficiencies in canopy point clouds. The accuracy and scanning distance constraints of HMLS make it difficult to accurately capture the full forest structure from the restricted canopy point cloud data. Although HMLS can penetrate gaps between leaves, dense canopies can lead to imbalances or deficiencies in canopy point clouds, especially in the upper sections of trees, making it challenging to estimate key forest parameters.

To address the limited canopy point clouds and understory effects, a common limitation of the HMLS LiDAR system, current practices involve fusing LiDAR data from multiple platforms[27,28]. This approach generates a comprehensive and holistic point cloud dataset. Typically, this process combines ground-based LiDAR, which scans from the forest floor upwards, with aerial LiDAR capturing data from the canopy downwards. Through advanced fusion techniques, this integration significantly improves the accuracy of estimating forest parameters. For instance, with the consolidated point cloud data, breast diameter measurements can be precisely determined using techniques such as the Hough transform circle detection, convex hull algorithm, least squares method, and cylinder fitting. Similarly, tree height can be accurately calculated by subtracting the coordinates of the top and bottom points[29].

Combining LiDAR data from different platforms presents challenges in reconstructing tree stem curves, primarily due to variations in point cloud density and scan angles, which can result in registration errors affecting the precision of forest parameter measurements[30,31]. Moreover, the limited overlap between ground and aerial data, especially in intricate forest terrains, adds complexity to point cloud registration, thereby raising uncertainty levels. While the dual-platform approach improves forest resource surveys, it also increases time and labor expenses.

Regardless of the type of LiDAR point cloud employed, the underlying approach remains fundamentally data-driven for forest parameter retrieval, often overlooking the inherent growth patterns and biological characteristics of trees and forest stands. In contrast, forest sciences offer well-established structural and process-based knowledge that captures physiological constraints and developmental relationships governing stem form and stand dynamics. Examples include stem taper models such as the Kunze curve[32] and stand-level DBH-height relationships. This domain knowledge provides an essential context for interpreting purely data-driven methods of forest parameter extraction. Effectively integrating the two is key to achieving accurate and ecologically meaningful estimation of forest attributes, which not only harness the strengths of large-scale point cloud data, but also incorporates existing silvicultural and growth models. Consequently, the fusion of tree- and stand-level models with LiDAR point cloud data represents a major focus of contemporary research.

In response to the practical limitations of HMLS point clouds in areas with insufficient canopy penetration, this study proposes a hybrid strategy that integrates stem taper modeling, an allometric H-D (height-diameter) growth model, and HMLS data to explore. By relying solely on low-density and partially occluded HMLS point clouds, the method achieves complete estimation of tree height and volume through partial stem fitting combined with model-based height compensation. The approach demonstrates stable performance across both natural and plantation forests. Using plots across the subtropical zone in Shengnongjia Forest Park, the study aimed to address two specific questions: (1) how can the stem curve be reconstructed using forest models and HMLS laser data? and (2) what is the performance of this approach in both planted and natural forests?

Methods and materials

Study area

The study was conducted in the Shennongjia Forest area (31°15' N–31°57' N, 109°56' E–110°58' E), located in the western part of Hubei Province, China (Fig. 1). The Shennongjia Forest area is one of the richest areas of endemic genera in China, with considerable biodiversity. The forest area has diversity topographic environment, the elevation ranges from 1,500 m to 3,105.4 m, and contains high mountains and steep slopes. The dominant tree species are *Pinus armandii*, *Cunninghamia*, *Larix gmelinii Abies fargesii*, *Quercus glauca*, and *Betula albosinensis*.

Data collection

Field data

The field work was carried out from August 25 to September 30 2022 with square plots. In total, 12 plots were collected across study regions. Considering the species composition and origin of the forest, the plots can also be divided into planted broad-leaved (PB), planted coniferous (PC), natural mixed broad-leaved (NB), and natural mixed coniferous (NC) forest stands. The plot size was set to 30m × 30 m. In each plot, we collected the position of each individual tree by a Postex laser sonar locator (Haglöf Sweden AB, Sweden). DBH was measured by a breast diameter ruler for trees with DBH > 5 cm, and the height of each tree was measured by a Vertex IV Hypsometer (Klockargatan, Sweden), and the corresponding species was recorded (Table 1).

HMLS data

HMLS point cloud data was performed using the ZEB-Revo handheld LiDAR scanner (GeoSLAM, UK), which consists of a 2D laser scanner with a field view of 360 × 270°, combined with an inertial measurement unit (IMU). The scanner operates at a rate of 43,200 points per second with a 100 Hz line speed, and a measurement range of 30 m. To ensure high-quality data in dense forest environments, we focused on the effective range of 15–20 m[22,33]. In order to avoid the missing points in collecting, we maintained a constant walking speed of approximately 0.5 m/s along an 'S' trajectory to ensure comprehensive coverage. The start and end points were coincident to form a closed loop for the SLAM matching algorithm[22] (Fig. 2). Each plot took approximately 20 min to scan.

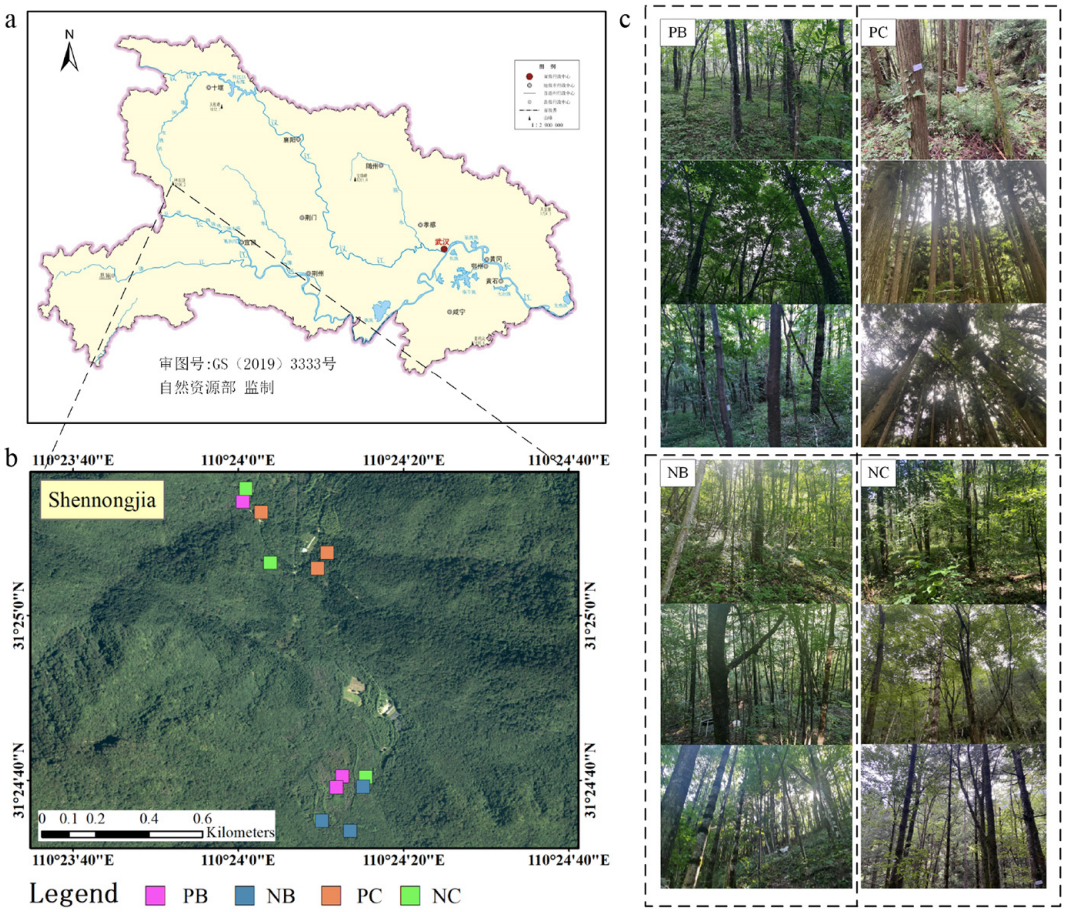

Fig. 1 Spatial distribution of different complex plots with various forest types. (a) Location of study area in Hubei; (b) plots in subtropical zone, located in Shennongjia, Hubei Province; (c) on-site photos of the 12 plot forest types with different complexity levels; PB and PC represents the planted broad-leaved and planted coniferous forest with a small amount of understory and medium visibility, respectively; NB and NC represent the natural mixed broad-leaved forest, and the natural mixed coniferous forest, with a large amount of understory and poor visibility. Source: http://bzdt.ch.mnr.gov.cn/index.html

Table 1. Information from forest plot surveys of varying complexity.

Plot ID	Characteristics of plots	Number of trees	Stem density (stems/ha)	DBH (cm)	Height (m)	Slope (°)	Canopy cover	Stem volume (m^3)	Stand volume (m^3/ha)
1	PB	69	767	15.6 ± 11.1	10.5 ± 5.1	18	0.7	0.27 ± 0.69	141.1
2	PB	66	733	18.5 ± 12.8	10.9 ± 5.6	16	0.8	0.28 ± 0.50	140.7
3	PB	56	622	17.1 ± 10.7	10.4 ± 5.3	14	0.5	0.22 ± 0.44	79.2
4	PC	60	667	26.2 ± 10.2	17.5 ± 6.7	21	0.7	0.66 ± 0.61	429.3
5	PC	61	678	28.8 ± 6.9	16.2 ± 5.3	23	0.8	0.54 ± 0.39	355.1
6	PC	56	622	30.8 ± 8.2	21.0 ± 7.3	25	0.6	0.89 ± 0.55	518.3
7	NB	78	867	19.7 ± 11.9	12.7 ± 5.2	16	0.7	0.36 ± 0.57	206.3
8	NB	61	678	21.1 ± 14.6	13.9 ± 6.7	17	0.6	0.54 ± 1.13	152.4
9	NB	48	533	25.4 ± 16.2	11.6 ± 6.1	13	0.5	0.54 ± 1.15	91.5
10	NC	82	911	25.1 ± 9.7	15.0 ± 7.3	20	0.6	0.49 ± 0.50	410.7
11	NC	56	622	21.1 ± 8.2	12.8 ± 4.5	22	0.7	0.30 ± 0.39	158.0
12	NC	88	978	21.9 ± 9.4	12.5 ± 5.3	26	0.8	0.36 ± 0.57	203.1

Note: plot characteristics are defined by origin (P: planted, N: natural), and forest type (B: broad-leaved, C: coniferous).

To determine the boundaries of the study area and the positions of individual trees, nine evenly spaced target spheres with a height of 1.3 m were inserted into the ground at the designated locations within the study site (Fig. 2). The raw data collected by ZEB-Revo (GeoSLAM, UK) were processed with the software GeoSLAM Hub, which used the simultaneous localization and mapping algorithm to locate the scanner in an unknown environment and register the whole 3D point clouds[34]. The average raw point density across the 12 plots reached approximately 3,500 pts/m^2.

Methods

The point cloud acquired by HMLS may have some occlusion, limiting the acquisition of tree height (Fig. 3). To solve this problem, we proposed a workflow (Fig. 4) to reconstruct stem and stand information. In summary, this integrated approach involves four steps: stem segmentation to extract the main stem point cloud; using Kunze's relative stem taper curve to construct tree stems; rebuilding an H-D model at the stand level to calculate tree heights that could not be constructed earlier; and finally, calculating forest attributes at

https://doi.org/10.48130/smartfor-0026-0008

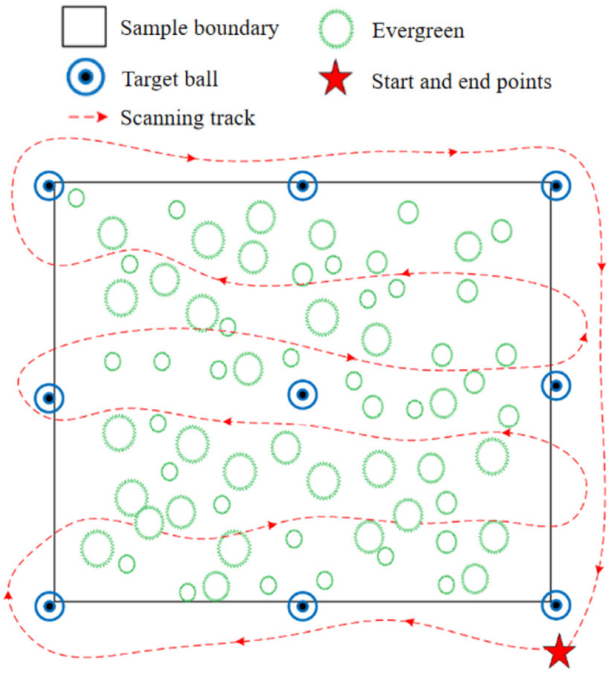

Fig. 2 Schematic diagram of the handheld LiDAR scanning path.

both the tree and stand level. From Fig. 4, the first stand cloud points data was collected by HMLS. After performing stem segmentation from step (a) to step (b), partial trunk point clouds can be extracted, facilitating the estimation of diameters at specific height levels. By combining this data with a stem curve model like Kunze's relative stem taper curve[32], a stem curve model can be created using discrete diameter measurements at corresponding heights. Although the goal is to construct trunk morphology curves, challenges such as trunk segmentation errors, diameter extraction errors, irregular tree distribution, topographical variability, and occlusion can hinder this process. For trees that cannot be reconstructed using stem point clouds, a regional height-diameter allometric growth model (H-D) was developed based on results from step (b) to predict missing tree heights, following a generalized approach commonly used in forestry stand surveys.

Ground and non-ground points separation

In order to enhance the computational efficiency of HMLS point cloud data, preprocessing was conducted. Due to variations in vegetation growth, height, and direction caused by different terrain, a cloth simulation filter (CSF) method is employed for ground separation and height normalization of the point cloud,with a cloth resolution of 0.5 m, a maximum of 500 iterations, and a classification threshold of 0.1 m[35]. Considering the localization errors of SLAM-based systems in forest environments, a statistical outlier removal method is employed to denoise the point cloud, eliminating measurement outliers and associated errors through parameterized filtering, with the number of neighboring points set to 30, and a standard deviation multiplier of 2.0[36].

Stem segmentation

To construct the trunk stem of every single tree, it is essential to extract numerous point clouds from the trunk to minimize occlusion effects. Various methods were synthesized for trunk extraction using ground-based LiDAR. For datasets with limited crown point clouds, a region-growing method was employed to automatically extract trunk point clouds. This method involves identifying seed points and growing rulers with these seeds[18,37]. Initially, point features such as curvature and vertical angle index in the point cloud were computed using k-nearest neighborhood[38]. Subsequently, seed points were generated using the density-based spatial clustering of applications with the noise (DBSCAN) algorithm. Horizontal slice points with a 10 cm thickness at a specific height were obtained from the original point cloud data and clustered using DBSCAN based on curvature and vertical angle indexes to identify potential trunks. Unlike Zhang's approach[37], our method classifies points in clusters as trunks if they exhibit low variation and a smaller flatness index, indicating more cylindrical and vertically consistent structures that are typical of tree stems[39]. Points most likely belonging to trunks are then extracted. Finally, a region growing algorithm was applied for trunk point cloud extraction[40]. A hypothesis is proposed that suggests points in the neighborhood surrounding the seed point exhibit similar curvature and vertical angles as the seed point. These neighboring points are merged into the same group as the seed point, while new points continue to expand in all directions from the seed. Horizontal growth is constrained within a fixed range (< 15 cm), with vertical growth being the primary direction. Ultimately, points within each group are considered part of the stem.

Diameter extraction at different heights

Starting from the base of the stem point clouds, horizontal slices with a thickness of 10 cm were extracted at 0.5 m intervals to determine diameter. A random sample consensus (RANSAC) cylinder fitting algorithm was utilized to fit the diameter by detecting cylindrical shapes based on the spatial distribution patterns of the

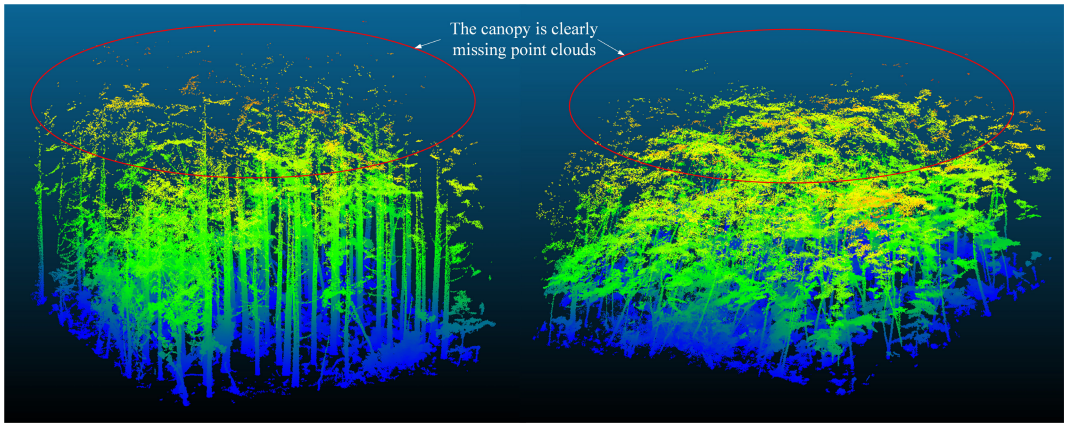

Fig. 3 Illustration of upper-canopy occlusion in point clouds acquired by HMLS.

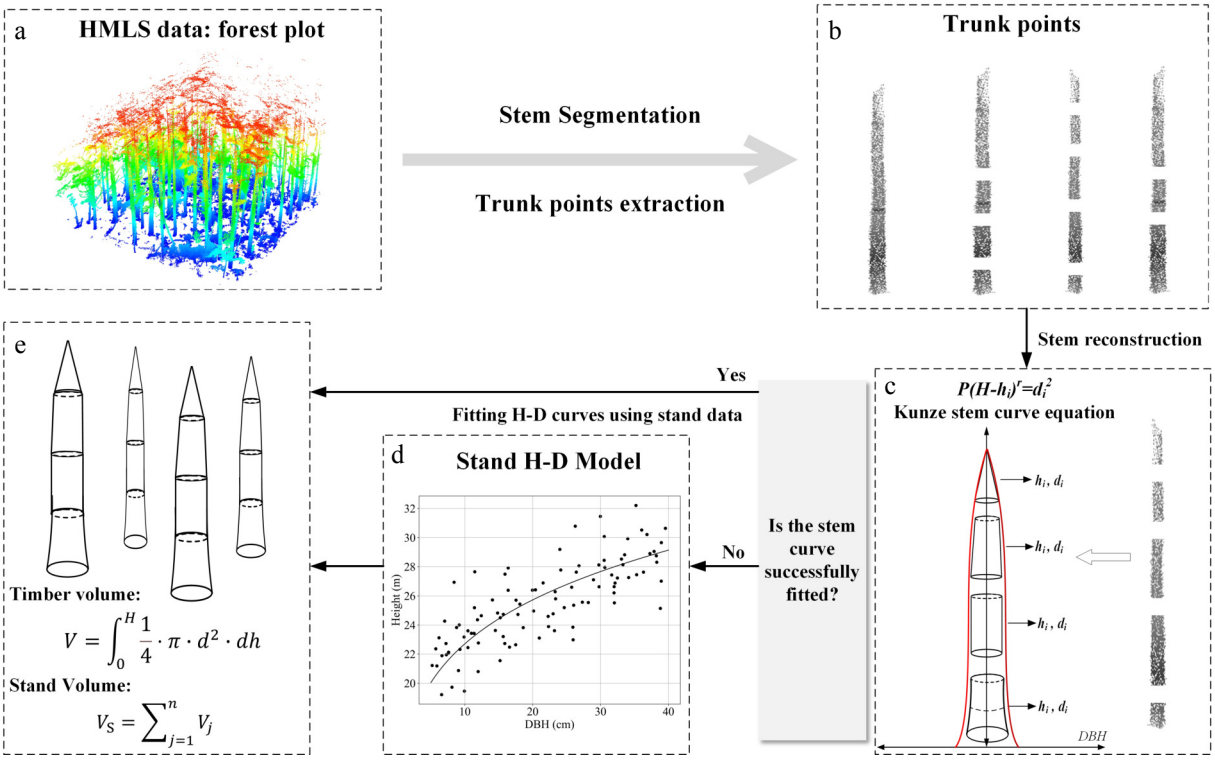

Fig. 4 Flowchart of the proposed method: (a) HMLS point cloud of forest plot with occlusions; (b) stem segmentation and trunk points extraction; (c) stem reconstruction using Kunze's stem curve equation; (d) stand H-D model development; (e) timber and stand volume calculation.

point cloud. This approach addresses the limitations of two-dimensional DBH estimation methods, which struggle to accurately estimate DBH when trees are tilted[41]. Specifically, the DBH was determined in a similar manner, and if the point cloud at 1.3 m was obscured, it was estimated through linear interpolation using the two nearest diameters at 1.3 m. The DBH values were then interpolated with the closest diameters. This process resulted in a collection of diameters and their corresponding heights, which will be used to construct the tree stem curve.

Stem curve modeling

Tree trunks typically exhibit cylindrical and parabolic forms, with minimal concave curve bodies and cones. Comparison of individual tree trunk point clouds with rotational bodies showed a predominant parabolic shape, with trunks being thicker at the base and tapering towards the canopy. The Kunze taper model features a concise functional form and requires only a small number of parameters to describe the tapering of the stem from base to top, making it well-suited for estimation under limited HMLS point cloud conditions where the full stem cannot be captured. Moreover, the model has been widely applied in stem reconstruction studies at the individual tree level, demonstrating strong adaptability[32]. This study utilized Kunze's relative stem taper curve for analysis (Eq. [1]):

$$d_i^2 = P(H - h_i)^r \quad (1)$$

where, P is an undetermined coefficient, H is the tree height, d_i and h_i are diameter and corresponding height, respectively, and r is the shape index of the tree. In this study, r is set to 1, as this value effectively captures the parabolic taper characteristics commonly observed in upright trees. Additionally, this setting reduces the number of fitting parameters, helping to prevent overfitting and improve computational efficiency[42].

The parameters P and H are estimated from curve fitting. Using cross-sectional diameter d_i at height h_i extracted from the point cloud data of the tree trunk (Fig. 4d), these values are then combined in the equation to fit the optimal curve of the tree trunk and determine the tree height H. To account for errors in diameter extraction using the cylinder fitting algorithm method, we employed a gross error stepwise elimination algorithm (GESEA). The main steps are as follows:

(1) Fit Eq. (1) with the d_i and h_i sequence, calculate the root mean square error (RMSE), and identify errors in each d_i;

(2) If RMSE is less than or equal to T, return the fitted result. According to existing literature on DBH estimation using TLS, an RMSE of ≤ 2.0 cm is widely regarded as an acceptable level of fitting accuracy; therefore, T is set to 2.0[43];

(3) If RMSE is exceeding T, eliminate the diameter with the largest error from the d_i, h_i sequence;

(4) Repeat step 1.

While Kunze's model can partially address the challenges of fitting tree height under high canopy closure conditions, where treetop cloud points are missing, certain trees may still pose difficulties due to their irregular growth or errors in extracted diameter and height data. A broader vertical coverage of the stem—especially when including segments close to the treetop—provides more constraints for curve extrapolation and leads to better height predictions. In contrast, when the upper portion of the stem is missing due to occlusion or low point density, the extrapolation becomes more dependent on the assumed taper model and may introduce bias. We ensured the fitting quality by using RMSE and retained only those curves with RMSE ≤ 2.0 m[44]. These combined constraints help reduce uncertainty and improve the robustness of the estimated tree height.

To account for the impact of site conditions on stand tree height, we developed an H-D model specifically for plots with similar stand conditions, using data from well-fitted stem curve trees. The H-D model was constructed using trees with complete point clouds as a representative subset of the stand. Since these trees share the same

site conditions with the occluded trees within the same plot, the localized H-D relationship remains biologically valid for height compensation. This model was employed to estimate the tree heights of trees that could not be directly fitted to stem curves using point cloud data. In our study, we opted for a hyperbolic model to redefine the H-D relationship (Eq. [2]), and the parameters (a_1, a_2, a_3) were estimated using the non-linear least squares (NLS) method to ensure the best fit between tree height and DBH data. Despite potential errors in tree height estimation across different species, this metric can capture the overall influence of site conditions on tree height growth, serving as an indicator of average stand height[45]. Once tree height is determined, it can be incorporated into Eq. (1) to reconstruct a model for individual trees:

$$H = a_1 - \frac{a_2}{DBH + a_3} \tag{2}$$

where, H is the tree height, DBH is the diameter at breast height, a_1, a_2, and a_3 are parameters to be solved.

Forest attribute estimation

By substituting the Kunze taper equation (Eq. [1]) into the standard sectional integration formula, the stem volume is calculated. The individual tree volume is then estimated with Eq. (3), ultimately leading to the calculation of stand volume for a single plot using Eq. (4).

$$V = \int_0^H \frac{1}{4} \cdot \pi \cdot d^2 \cdot dh = \frac{\pi}{4} P \int_0^H (H-h)^r \cdot dh \tag{3}$$

$$V_s = \sum_{j=1}^{n} V_j \tag{4}$$

where, V is the volume of individual wood, V_s is the stand volume, H is the tree height, P is the the fitting parameters in Eq. (1), d is the stem diameter at height h.

Accuracy assessment

At the individual and stand level, the field data was used to assess the performance of the proposed method. The tree detection rate, the errors of DBH, tree height, the individual timber volume and stand volume were evaluated with the following statistical analysis. The tree detecting rate (DR) and commission rate (CR) were used for evaluating the accuracy of tree detection, which were defined as Eqs (5) and (6). The coefficient of determination (R^2), RMSE, relative RMSE (rRMSE), MAE, relative MAE (rMAE), bias, and relative bias (rbias) were utilized as evaluation metrics for DBH, tree height, individual tree volume, and stand volume, which were defined in Eqs (7)–(13).

$$DR = N_{rd} \,/N_r \tag{5}$$

$$CR = 1 - N_{rd} \,/N_t \tag{6}$$

where, N_{rd} is the number of reference trees found within our method, N_r is the total number of reference trees, and N_t is the total number of trees found within our method.

$$R^2 = 1 - \frac{\sum_{i=1}^{n} (y_i - \hat{y}_i)^2}{\sum_{i=1}^{n} (y_i - \bar{y})^2} \tag{7}$$

$$\text{bias} = \frac{\sum_{i=1}^{n} (\hat{y}_i - y_i)}{n} \tag{8}$$

$$\text{rbias} = \frac{\text{bias}}{\bar{y}} \tag{9}$$

$$\text{MAE} = \frac{\sum_{i=1}^{n} |\hat{y}_i - y_i|}{n} \tag{10}$$

$$\text{rMAE} = \frac{\text{MAE}}{\bar{y}} \times 100\% \tag{11}$$

$$\text{RMSE} = \sqrt{\frac{\sum_{i=1}^{n} (y_i - \hat{y}_i)^2}{n}} \tag{12}$$

$$\text{rRMSE} = \frac{\text{RMSE}}{\bar{y}} \times 100\% \tag{13}$$

where, n is the number of matched trees, $\hat{y}_i$ is the estimated value of DBH, tree height, timber volume, and stand volume, y_i is the corresponding reference value, and $\bar{y}$ is the mean value of reference value.

Comparison with the conventional method

To evaluate the optimization effect of the integrated approach, a comparative analysis was conducted against the conventional direct extraction method using LiDAR360 software (v9.0, GreenValley International). This comparison was specifically limited to the subset of trees for which stem curves were successfully fitted. This selection was necessary because conventional methods rely on sufficient point cloud visibility of the tree apex; for trees with severe canopy occlusion, these methods typically fail to detect the individual trees, or produce invalid height measurements[29,46]. By comparing the two methods on this fitted subset, we aimed to quantify the accuracy improvement provided by stem taper modeling over standard point-to-point extraction. In LiDAR360, individual tree segmentation (ITS) was performed using a search radius of 1.0 m and a minimum height threshold of 2.0 m.

Results

Accuracy of tree detection and DBH extraction

The evaluation of single tree detection rate and DBH accuracy was conducted across all plots initially. Table 2 provides a detailed overview of the DBH accuracy metrics for each plot. The HMLS data exhibited a high efficacy in tree detection within the sample plots, with detection rates exceeding 91% in most cases and commission error rates below 10%. Plot 10 demonstrated the highest forest tree detection accuracy, with a detection rate of 98.68% and a commission error rate of 1.23%. In contrast, plot 9 displayed the lowest accuracy, with a detection rate of 86.05% and a commission error rate of 14.29%. The R^2 values for detected DBH and measured DBH surpassed 0.94 across all plots, except for plot 12, where the R^2 value was 0.89. The bias ranged from a maximum of 0.76 cm (plot 12) to a minimum of 0.02 cm, with only two plots showing negative bias values, indicating an overestimation of DBH by the HMLS data in most cases. The Mean Absolute Error (MAE) for all plots was less than 1.2 cm, and the relative MAE (rMAE) generally remained below 5%, except for plots 3, 11, and 12, where the rMAE values were 7.26%, 5.58%, and 5.47%, respectively. The Root Mean Square Error (RMSE) for all sample plots was under 2.2 cm, with the relative RMSE (rRMSE) falling within 10%, except for plots No. 3 and No. 12, which had rRMSE values of 10.71%, and 10.47%, respectively. The scatter statistical analysis comparing the DBH extracted by HMLS with the field-measured DBH across all plots revealed a strong correlation (Fig. 5a) with an R^2 value of 0.98. The bias and relative bias were 0.3 cm, and 1.28%, respectively, indicating an overestimation of diameter by HMLS (Fig. 6a) across all forest types. Additionally, the MAE and relative MAE were 0.7 cm, and 3.57%, respectively, while the RMSE and relative RMSE were also relatively small, at 1.5 cm, and 7.32%, respectively. These findings highlight a high level of agreement and accuracy between the estimates obtained from LiDAR data and the actual field measurements.

Accuracy of tree height

We compared tree height estimation using two methods: the stem curve model (Table 3) and the H-D model (Table 4). Stem curve construction rates varied across plots, with a maximum of 91.89% in plot 9 and a minimum of 42.62% in plot 1, both in planted forests. Natural forests (plots 7–12) also showed varying stem curve construction rates, ranging from 54.00% to 91.89%. Plot 9 had the highest successful construction rate at 91.89%, with an estimated tree height R^2 value of 0.97, MAE of 0.62 m, and rMAE of 6.09%, indicating high accuracy. On the other hand, plot 1 had the lowest successful construction rate at 42.62%, with an R^2 value of 0.90, MAE of 1.20 m, and rMAE of 12.89%. Sample plots 2 and 3 had similar successful construction rates of 83.93% and 84.00%, with comparable estimation accuracy metrics. Sample plots 6 and 9 also showed similar characteristics, both with higher R^2 values, and lower MAE values. Despite a low construction rate of 55.71%, sample plot 7 displayed relatively high estimation accuracy. Sample plots 5 and 10 had comparable R^2 values, MAEs, and rMAEs. Overall, R^2 values

Table 2. The accuracy of DBH in each plot.

Plot ID	DR (%)	CR (%)	R^2	bias (cm)	rbias (%)	MAE (cm)	rMAE (%)	RMSE (cm)	rRMSE (%)
1	91.04	9.52	0.98	0.13	0.90	0.67	4.60	1.31	8.95
2	91.80	8.20	0.99	0.16	0.99	0.31	1.93	0.66	4.15
3	94.30	5.66	0.96	−0.09	−0.57	1.10	7.26	1.63	10.71
4	98.31	1.69	0.97	0.41	1.57	1.05	4.00	1.97	7.53
5	98.31	1.67	0.97	0.51	1.95	0.94	3.58	1.78	6.81
6	96.30	3.70	0.97	0.08	0.27	0.67	2.18	1.31	4.27
7	95.89	4.00	0.98	0.02	0.12	0.54	3.09	1.27	7.22
8	88.89	10.91	0.99	0.02	0.12	0.11	0.61	0.20	1.11
9	86.05	14.29	0.99	−0.08	−0.42	0.21	1.08	0.55	2.82
10	98.68	1.23	0.94	0.67	2.75	1.18	4.81	2.12	8.66
11	96.15	3.70	0.94	0.29	1.43	1.11	5.58	1.88	9.45
12	96.20	3.53	0.89	0.76	3.76	1.11	5.47	2.12	10.47

Note: DR represents detection rate; CR represents commission rate.

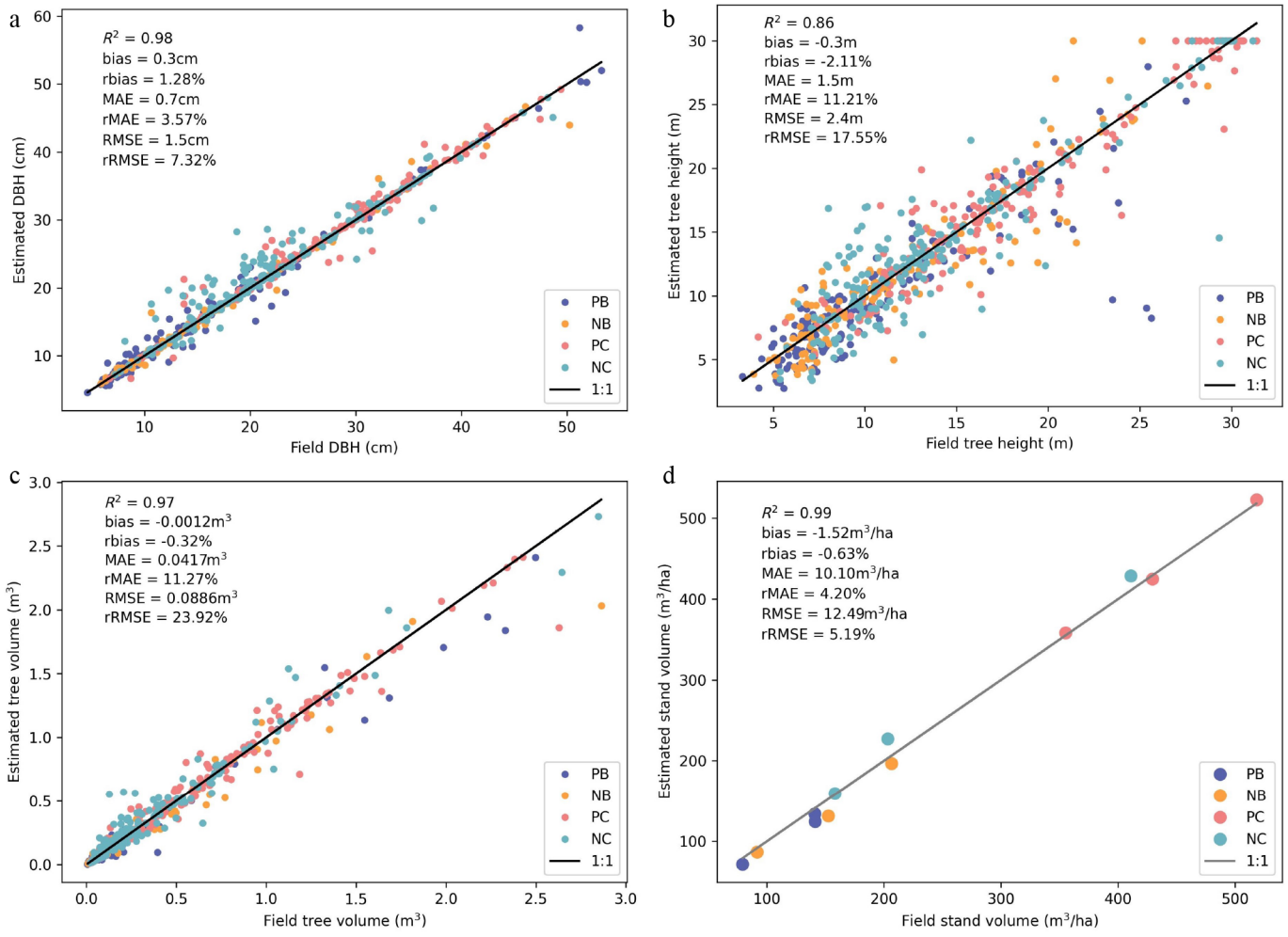

Fig. 5 Scatter plots of LiDAR-extracted forest attributes vs measured forest attributes across plots: (a) diameter at breast height (DBH), (b) tree height, (c) stem volume, and (d) stand volume.

https://doi.org/10.48130/smartfor-0026-0008

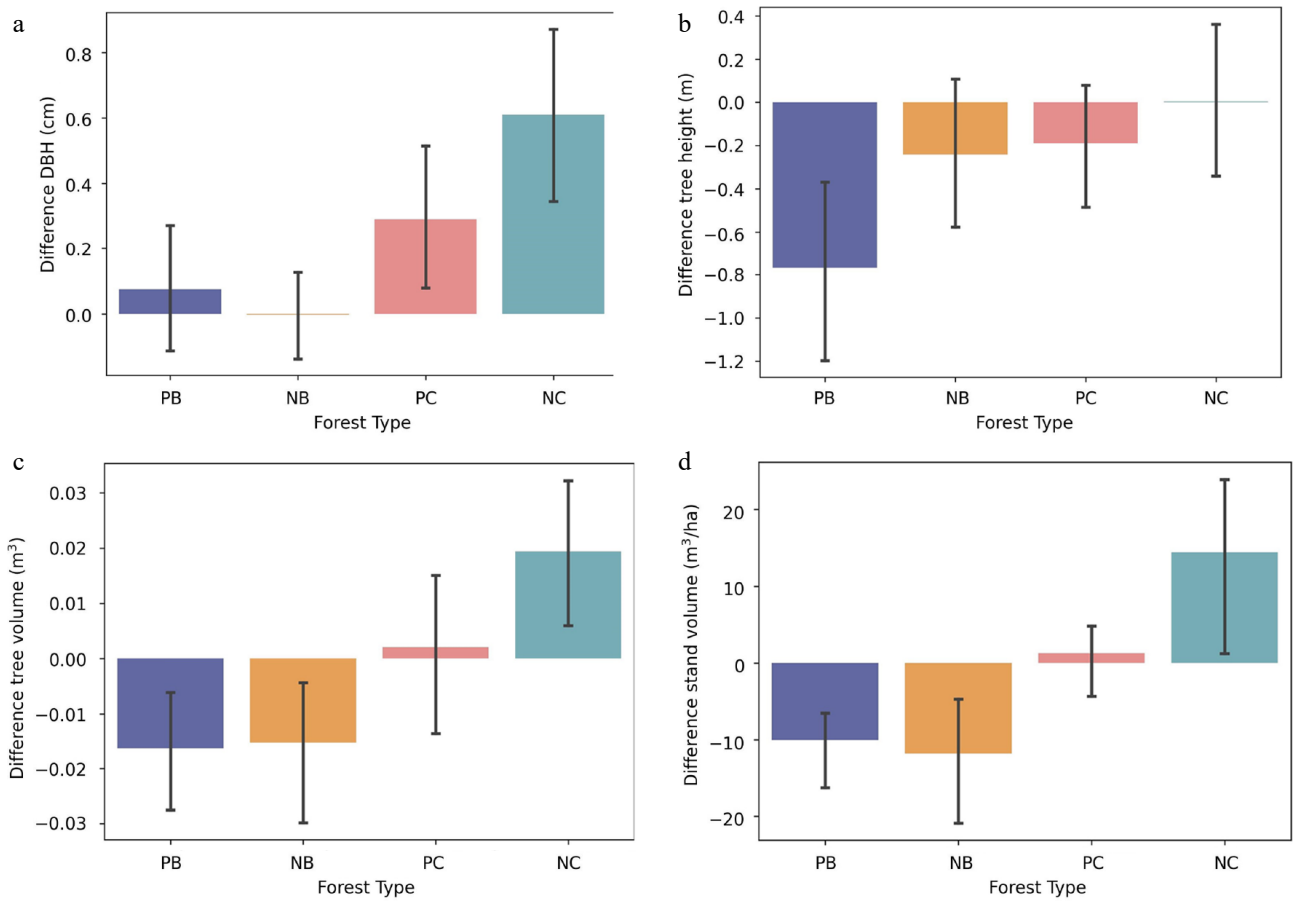

Fig. 6 Bar plots of bias errors for LiDAR-extracted vs measured forest attributes across plots: (a) diameter at breast height (DBH), (b) tree height, (c) stem volume, and (d) stand volume.

ranged from 0.80 to 0.97, indicating high accuracy and reliability of the stem curve construction method in tree height estimation. The average RMSE of tree height was lower than 1.5 m.

Table 4 presents the accuracy of tree height estimates using the H-D model at the stand level, aiding in estimation of tree heights not derived from the stem curve model. Notably, sample plot 1 demonstrates the highest accuracy in tree height estimation, with an R^2 value of 0.78, MAE of 1.33 m, rMAE of 12.67%, and rRMSE of 19.80%, indicating its precise estimation results. Conversely, sample plot 2 exhibits the lowest accuracy, with an R^2 value of 0.25, a high MAE of 5.25 m, rMAE of 39.64%, and rRMSE of 61.72%, highlighting significant errors in its height estimation. Sample plot 7 also shows relatively high accuracy, with an R^2 of 0.68, deviation of 0.41 m, and rMAE of 13.54%. In contrast, sample plot 3 displays poor accuracy, with an R^2 value of 0.04, MAE of 3.60 m, and rMAE of 29.10%, indicating its ineffective estimation. The R^2 values for plots 5, 6, 8, 9, 10, and 12 fall between 0.27 and 0.50, with MAE ranging from 2.55 to 3.92 m, suggesting a moderate level of accuracy in estimating tree heights for these plots.

Figure 5b displays a scatter plot comparing the extracted tree height with the field-measured tree height. The statistical analysis reveals a strong correlation between the two with an R^2 value of 0.86. The bias is calculated to be −0.3 m, rbias at −2.11%, MAE recorded at 1.5 m, rMAE at 11.21%, RMSE at 2.4 m, and rRMSE at 17.55%. These findings suggest that while there may be some discrepancies between the estimated tree height from extraction and the actual field measurements, overall the accuracy and consistency are satisfactory. However, the underestimation of tree height by HMLS is a universal phenomenon across all forest types (Fig. 6b).

Individual wood volume estimation

The stem volume estimates derived from HMLS data demonstrated high accuracy and consistency with field measurements across most plots, with (R^2) values generally exceeding 0.94, except for plots 3 and 12. Overall, HMLS tended to underestimate stem volume, particularly in high volume ranges and in broad-leaved forests, while slightly overestimating in coniferous forests. Notably, plots 2 and 5 exhibited the highest estimation accuracy, both achieving (R^2) values of 0.98, indicating excellent agreement between HMLS estimates and field measurements. In contrast, plot 12 had the lowest accuracy $(R^2 = 0.77)$, suggesting more significant

Table 3. The accuracy of tree height from stem curve constructed in plots.

Plot ID	Successful stem curve constructed rate (%)	Tree height for stem curve constructed						
		R^2	bias (m)	rbias (%)	MAE (m)	rMAE (%)	RMSE (m)	rRMSE (%)
1	42.62	0.90	−0.20	−2.14	1.20	12.89	1.41	15.09
2	83.93	0.89	−0.61	−5.77	1.36	12.79	1.63	15.39
3	84.00	0.89	−0.56	−5.67	1.35	13.72	1.58	16.06
4	81.03	0.97	−0.17	−0.97	0.92	5.23	1.21	6.92
5	82.76	0.95	−0.34	−2.05	0.90	5.48	1.23	7.45
6	88.46	0.97	0.04	0.20	0.95	4.45	1.28	5.97
7	55.71	0.80	0.24	1.80	1.74	13.07	2.64	19.83
8	64.58	0.94	−0.44	−3.92	1.15	10.19	1.45	12.86
9	91.89	0.97	−0.34	−3.29	0.62	6.09	0.96	9.40
10	74.67	0.97	−0.06	−0.36	0.94	5.88	1.37	8.64
11	54.00	0.93	−0.62	−4.59	0.88	6.50	1.35	9.94
12	64.47	0.86	−0.59	−4.91	1.14	9.47	1.54	12.76

Table 4. The accuracy of tree height from stand H-D model in plots.

Plot ID	Tree height from H-D model						
	R^2	bias (m)	rbias (%)	MAE (m)	rMAE (%)	RMSE (m)	rRMSE (%)
1	0.78	−0.71	−6.75	1.33	12.67	2.08	19.80
2	0.25	−3.28	−24.75	5.25	39.64	8.18	61.72
3	0.04	−2.07	−16.69	3.60	29.10	5.42	43.82
4	0.41	−2.18	−12.18	3.27	18.31	3.67	20.53
5	0.30	0.73	4.78	2.95	19.20	3.73	24.25
6	0.27	1.17	6.91	2.55	15.00	3.45	20.32
7	0.68	0.41	3.84	1.46	13.54	1.96	18.19
8	0.50	−1.80	−12.38	3.29	22.59	3.65	25.10
9	0.06	−2.87	−19.22	3.92	26.28	4.65	31.17
10	0.36	0.71	5.02	3.61	25.55	4.91	34.75
11	0.60	−0.10	−0.80	2.38	18.65	3.02	23.61
12	0.33	1.43	12.26	2.72	23.32	3.61	30.96

discrepancies in this plot. Plots 9 and 10 also showed high accuracy (R^2) values of 0.97 and 0.96, respectively, further supporting the reliability of HMLS for stem volume estimation in most cases (Table 5). These results highlight the varying performance of HMLS across different forest types (Fig. 6c), with generally good accuracy in coniferous forests and more variability in broad-leaved forests.

A scatter plot in Fig. 5c illustrates the relationship between estimated stem volume and field-measured stem volume. The statistical analysis reveals a strong correlation with an R^2 value of 0.97. Additionally, there is a slight bias of −0.0012 m^3, rbias of −0.32%, MAE of 0.0417 m^3, rMAE of 11.27%, RMSE of 0.0886 m^3, and rRMSE of 23.92%. These findings indicate a high level of agreement and accuracy between the estimated trunk volumes and the field measurements.

Stand volume estimation

The accuracy of stand volumes across 12 plots was seen in Fig. 5d. The correlation between the estimated and measured stand volume was high, with R^2 of 0.99, the bias and rbias were −1.53 m^3/ha and −0.63%, respectively, indicating that the stand volume estimated by HMLS data would be underestimated. The MAE and rMAE was 10.1 m^3/ha, and 4.20%, respectively. The RMSE and rRMSE were 12.49 m^3/ha, and 5.19%, respectively. However, it was also found that stand volume was underestimated in broad-leaved forest and overestimated in coniferous forest (Fig. 6d).

Comparison of accuracy across forest types

To assess methodological robustness, we aggregated data into four forest categories for statistical comparison (Table 6). Across all groups, DBH extraction remained highly stable, yielding R^2 values above 0.93, and rMAE below 6%. Specifically, the rRMSE in NB and PC was 5.10% and 5.19%, respectively, confirming that diameter retrieval is consistently reliable regardless of canopy complexity.

Conversely, tree height and volume estimations were more sensitive to forest structure. Planted coniferous forests (PC) achieved the highest accuracy, with an rRMSE of 10.18% for height and 13.88% for stem volume. The highest relative errors occurred in planted broad-leaved forests (PB), where the rRMSE for height and stem volume reached 26.47% and 39.11%, respectively, due to complex branch architectures and severe occlusion.

At the stand level, the estimation of stand volume was exceptionally reliable, particularly for coniferous stands where error metrics were consistently lower than those in natural forests. Overall, while the integrated approach effectively compensates for forest parameters when canopy information is difficult to obtain, its accuracy remains higher in simpler plantation structures than in diverse natural forests.

Table 5. The accuracy of stem volume in each plot.

Plot ID	Stem volume						
	R^2	bias (m^3)	rbias (%)	MAE (m^3)	rMAE (%)	RMSE (m^3)	rRMSE (%)
1	0.96	−0.0240	−11.55	0.03	15.91	0.0978	46.99
2	0.98	−0.0105	−4.65	0.03	11.44	0.0645	28.52
3	0.88	−0.0131	−9.19	0.03	19.52	0.0549	38.51
4	0.96	−0.0067	−1.01	0.06	8.69	0.1205	18.08
5	0.98	0.0052	0.95	0.03	6.32	0.0579	10.52
6	0.97	0.0083	0.93	0.06	6.84	0.1020	11.37
7	0.94	−0.0125	−4.71	0.04	13.44	0.1087	40.99
8	0.95	−0.0392	−13.70	0.05	17.48	0.1365	47.77
9	0.97	−0.0115	−5.15	0.02	8.82	0.0460	20.64
10	0.96	0.0218	4.43	0.06	12.60	0.1011	20.52
11	0.96	0.0022	0.78	0.04	15.32	0.0748	26.32
12	0.77	0.0283	11.77	0.05	20.52	0.0970	40.30

Comparison of the proposed and conventional method

Table 7 presents a comparative analysis of tree height estimation results obtained from the conventional direct extraction method using LiDAR360 and the proposed integrated approach. This comparison focuses exclusively on the subset of trees for which both methods yielded valid numerical estimates. Within this subset, the conventional method demonstrated a strong correlation with field-measured heights, achieving an R^2 value of 0.85. Nonetheless, it exhibited a systematic underestimation bias, with a mean bias of −0.3964 m and a relative bias (rbias) of −3.57%. These findings suggest that, even under relatively favorable conditions, standard point-to-point extraction algorithms frequently fail to accurately capture the true tree apex.

In contrast, the proposed integrated model substantially improved estimation accuracy. The coefficient of determination increased to 0.92, while the bias decreased to −0.1895 m and the rbias improved to −1.04%. Although the conventional method yielded a slightly lower absolute root mean square error (RMSE) of 0.8129 m within this specific subset, its principal limitation lies in a high omission rate, particularly in dense canopy environments. For trees subject to severe occlusion, LiDAR360 was unable to extract

Table 6. The accuracy for forest attributes across four forest types.

Attribute	Forest type	R^2	bias	rbias (%)	MAE	rMAE (%)	RMSE	rRMSE (%)
DBH	PB	0.98	0.08	0.50	0.68	4.46	1.25	8.21
	PC	0.97	0.29	1.05	0.71	2.55	1.44	5.19
	NB	0.99	0.00	−0.02	0.33	1.86	0.90	5.10
	NC	0.93	0.61	2.81	1.13	5.22	2.06	9.49
Tree height	PB	0.70	−0.77	−7.37	1.64	15.77	2.76	26.47
	PC	0.93	−0.19	−1.04	1.26	6.91	1.85	10.18
	NB	0.83	−0.24	−2.04	1.51	12.79	2.21	18.75
	NC	0.80	0.00	0.03	1.64	12.07	2.53	18.69
Stem volume	PB	0.97	−0.02	−8.34	0.03	14.96	0.08	39.11
	PC	0.97	0.00	0.30	0.05	7.31	0.10	13.88
	NB	0.95	−0.02	−6.47	0.03	13.20	0.08	36.02
	NC	0.95	0.02	5.61	0.05	15.24	0.09	27.09
Stand volume	PB	0.86	−10.04	−8.34	10.04	8.34	10.97	9.12
	PC	0.99	1.28	0.30	4.17	0.96	4.21	0.97
	NB	0.92	−11.77	−7.84	11.77	7.84	13.58	9.05
	NC	0.98	14.44	5.61	14.44	5.61	17.36	6.75

Units for bias, MAE, and RMSE correspond to the respective attributes: cm for DBH; m for tree height; m^3 for stem volume; and m^3/ha for stand volume. Other metrics (rbias, rMAE, and rRMSE) are expressed as percentages (%).

Table 7. Accuracy comparison for tree height estimation.

Method	R^2	bias (m)	rbias (%)	MAE (m)	rMAE (%)	RMSE (m)	rRMSE (%)
LiDAR 360	0.85	−0.40	−3.57	0.61	5.48	0.81	7.33
Integrated	0.92	−0.19	−1.04	1.26	6.91	1.85	10.18

valid height parameters. Conversely, the integrated approach addressed these data gaps by incorporating a stand-level height-diameter (H-D) model, thereby providing reliable height estimates. Consequently, the integrated method not only delivers a more biologically consistent fit for detected stems, but also enhances the overall completeness and reliability of forest inventories in complex terrain conditions.

Discussion

Potential of HMLS data for forest attribute extraction

HMLS has demonstrated significant potential in forest resource surveys due to its efficient data collection capabilities[47]. Previous research has indicated that handheld mobile LiDAR is commonly used to extract DBH parameters in forest surveys, showing good results in both artificial and natural forests. However, it is important to acknowledge that handheld mobile LiDAR systems may not achieve 100% accuracy in data extraction from all trees. Our study found instances of missed detections and errors in both artificial and natural forests, with detection errors influenced by the forest stand structure. Particularly in natural forests, the rate of missed and false detections tends to be higher, consistent with prior research. While some researchers have utilized handheld mobile LiDAR systems to extract tree height, most agree that this method faces challenges. Due to factors such as high canopy density and occlusion, obtaining a complete point cloud of the top of the trunk is often unfeasible, hindering accurate tree height extraction. However, our proposed method, which combines LiDAR point cloud data with a forest stem curve and a stand DBH tree height model has shown promising results in reconstructing the stem curve for tree height extraction. Across various forest stands, the root mean square error of tree height extraction can be kept below 2.4 m, with the average median error in artificial forests remaining within 1.5 m.

With a relatively accurate tree height, better results will be achieved in terms of single tree volume and stand accumulation. The study in this article also reveals that the root mean square error and relative root mean square error of single wood volume can be controlled at 0.0886 m^3 and 23.92%. When considering the volume of a single tree, broad-leaved forests tend to have an overall underestimation, while coniferous forests tend to have an overall overestimation. Artificial coniferous forests show the highest estimation accuracy for volume. This trend is also observed in forest stands and their storage. By integrating HMLS data with forestry models, we can effectively derive forest parameters in diverse terrain and stand conditions. This methodology is not only applicable to the specific study area but also holds promise for wider use in various forest types. The portable and flexible nature of HMLS equipment makes it well-suited for data collection in remote or challenging terrain forests, overcoming the constraints of conventional methods in such environments.

The effects of site and forest stand characteristics

Stand complexity represents a primary constraint on the accuracy of HMLS-derived forest attributes. Our study reveals significant disparities in extraction precision between planted and natural forests. In plantations, which are typically characterized by uniform tree spacing and single-species composition, the simpler canopy structure allows for more consistent laser pulse penetration and higher stem detection rates. Conversely, the structural diversity of natural forests leads to increased laser signal attenuation and irregular point cloud distribution.

This disparity is further accentuated by tree architectural differences. Notably, coniferous forests yielded more accurate height and volume estimations than broad-leaved forests. The intricate crown structures and spreading branches of broad-leaved species create severe occlusion zones, hindering the scanner from capturing the complete stem profile.

Furthermore, the undulating terrain and high vegetation density in mountainous plots significantly hindered signal reflection, resulting in reduced data accuracy. We found that while HMLS meets necessary standards for moderate-height trees, the estimation accuracy for trees exceeding 20 m decreases due to the limited scanning range and perspective of the handheld device. These findings underscore the importance of integrating modeling techniques to compensate for the inherent physical limitations of HMLS in topographically and biologically complex environments.

Factors influencing the accuracy of the stem curve model

The accuracy of extracting different height diameters significantly affects the modeling of dry curves. The irregular structure of forest stands and the shape of tree trunks play a crucial role in the extraction process. For example, in sample plots 3 and 6, the presence of curved trees in the forest greatly reduces the accuracy of trunk height extraction. Conversely, while the stems in plots 7, 8, and 9 are relatively straight, the abundance of side branches and twigs complicates complete removal during extraction, leading to significant discrepancies in trunk diameter and tree height accuracy. Furthermore, non-vertical tree growth affects the extraction of the section profile curve, resulting in discrepancies between actual and extracted trunk height changes, thereby impacting trunk curve fitting accuracy. Moreover, highly concentrated extracted diameters present challenges for direct fitting, with extraction errors affecting the overall fitting outcome.

Conclusions

HMLS is increasingly utilized for forest inventory because of its efficiency and convenience. However, extracting forest attributes remains challenging in complex stand structures where canopy occlusion limits point cloud penetration. To address these limitations, our method integrates two modeling approaches: Kunze's stem curve fitting for trees with clear trunk points, and stand-level H-D models to predict heights for trees with occluded canopies. This hybrid framework significantly improves the accuracy of stem and stand volume estimations compared to methods relying solely on raw point cloud geometry.

Specifically, our integrated approach is highly effective for forest inventory in rugged mountainous regions with high canopy closure, such as the Shennongjia Forest area. In these environments, the high density of foliage often leads to severe laser occlusion for both HMLS and aerial LiDAR, while steep slopes limit the use of heavy tripod-based scanners. Our method overcomes these challenges by using HMLS for rapid ground-level data acquisition and employing localized modeling to compensate for missing canopy information.

Our results indicate that estimation accuracy is highly sensitive to forest type, with plantations yielding higher precision than natural forests. This disparity is primarily due to the simpler stand structures and lower stem densities in plantations, which reduce signal occlusion and facilitate more robust stem segmentation. Furthermore, a consistent overestimation of DBH and underestimation of tree height were observed. The former is likely caused by point cloud thickness resulting from laser beam divergence and bark roughness, while the latter results from the terrestrial scanning geometry of HMLS, where dense foliage prevents the scanner from capturing the tree apex. Consequently, volume estimation errors varied; the height underestimation in broad-leaved forests led to a volume underestimation, whereas in coniferous forests, the DBH overestimation had a more pronounced impact on the final volume. Ultimately, this approach enhances the utility of handheld LiDAR in dense forests and supports the broader transition towards precision forest management and sustainable silvicultural practices.

Author contributions

The authors confirm their contributions to the paper as follows: conceptualization: Dian Y; methodology: Dian Y, Li ZL, Yang Z; software: Li ZL, Yang Z; formal analysis: Dian Y, Zhang Z, Li ZM; validation: Zhang Z, Zhou X, Guo Z; investigation: Guo Z, Hu L, Huang L; data curation: Li ZM, Li ZL, Hu L; writing – original draft: Zhang Z, Zhou X, Li ZL; writing – review and editing: Dian Y; visualization: Zhang Z, Zhou X, Huang L; supervision, project administration, funding acquisition, resources: Dian Y. All authors reviewed the results and approved the final version of the manuscript.

Data availability

The datasets generated during or analyzed during the current study are available from the corresponding author on reasonable request.

Acknowledgments

This research was funded by the National Natural Science Foundation of China (Grant No. 32071683), the Project of Fundamental Research Funds for the Central Universities (2662023YLPY003), and the Hubei Forestry Science and Technology Innovation Project (Grant No. [2025] LKZC11).

Conflict of interest

The authors declare that they have no known competing financial interests or personal relationships that could have appeared to influence the work reported in this paper.

Dates

Received 22 January 2026; Revised 26 March 2026; Accepted 17 April 2026; Published online 3 July 2026

References

[1] Baskent EZ. 2020. A framework for characterizing and regulating ecosystem services in a management planning context. *Forests* 11:102

[2] Del Perugia B, Giannetti F, Chirici G, Travaglini D. 2019. Influence of scan density on the estimation of single-tree attributes by hand-held mobile laser scanning. *Forests* 10:277

[3] Qin H, Zhou W, Yao Y, Wang W. 2022. Individual tree segmentation and tree species classification in subtropical broadleaf forests using UAV-based LiDAR, hyperspectral, and ultrahigh-resolution RGB data. *Remote Sensing of Environment* 280:113143

[4] Giannetti F, Chirici G, Travaglini D, Bottalico F, Marchi E, et al. 2017. Assessment of soil disturbance caused by forest operations by means of portable laser scanner and soil physical parameters. *Soil Science Society of America Journal* 81:1577–1585

[5] López Serrano FR, Rubio E, García Morote FA, Abellán MA, Picazo Córdoba MI, et al. 2022. Artificial intelligence-based software (AIDFOREST) for tree detection: a new framework for fast and accurate forest inventorying using LiDAR point clouds. *International Journal of Applied Earth Observation and Geoinformation* 113:103014

[6] Lu D, Chen Q, Wang G, Liu L, Li G, et al. 2016. A survey of remote sensing-based aboveground biomass estimation methods in forest ecosystems. *International Journal of Digital Earth* 9:63–105

[7] Guo Q, Su Y, Hu T, Guan H, Jin S, et al. 2021. Lidar boosts 3D ecological observations and modelings: a review and perspective. *IEEE Geoscience and Remote Sensing Magazine* 9:232–257

[8] Jin S, Sun X, Wu F, Su Y, Li Y, et al. 2021. Lidar sheds new light on plant phenomics for plant breeding and management: recent advances and future prospects. *ISPRS Journal of Photogrammetry and Remote Sensing* 171:202–223

[9] Zhao Y, Im J, Zhen Z, Zhao Y. 2023. Towards accurate individual tree parameters estimation in dense forest: optimized coarse-to-fine algorithms for registering UAV and terrestrial LiDAR data. *GIScience & Remote Sensing* 60:2197281

[10] Zolkos SG, Goetz SJ, Dubayah R. 2013. A meta-analysis of terrestrial aboveground biomass estimation using lidar remote sensing. *Remote Sensing of Environment* 128:289–298

[11] Calders K, Adams J, Armston J, Bartholomeus H, Bauwens S, et al. 2020. Terrestrial laser scanning in forest ecology: expanding the horizon. *Remote Sensing of Environment* 251:112102

[12] Liang X, Hyyppä J. 2013. Automatic stem mapping by merging several terrestrial laser scans at the feature and decision levels. *Sensors* 13:1614–1634

[13] Olofsson K, Holmgren J, Olsson H. 2014. Tree stem and height measurements using terrestrial laser scanning and the RANSAC algorithm. *Remote Sensing* 6:4323–4344

[14] Hyyppä E, Kukko A, Kaijaluoto R, White JC, Wulder MA, et al. 2020. Accurate derivation of stem curve and volume using backpack mobile laser scanning. *ISPRS Journal of Photogrammetry and Remote Sensing* 161:246–262

[15] Li YQ, Deng XW, Huang ZH, Xiang WH, Yan WD, et al. 2015. Development and evaluation of models for the relationship between tree height and diameter at breast height for Chinese-fir plantations in subtropical China. *PLoS One* 10:e0125118

[16] Dassot M, Constant T, Fournier M. 2011. The use of terrestrial LiDAR technology in forest science: application fields, benefits and challenges. *Annals of Forest Science* 68:959–974

[17] Hilker T, Coops NC, Culvenor DS, Newnham G, Wulder MA, et al. 2012. A simple technique for co-registration of terrestrial LiDAR observations for forestry applications. *Remote Sensing Letters* 3:239–247

[18] Liang X, Kankare V, Hyyppä J, Wang Y, Kukko A, et al. 2016. Terrestrial laser scanning in forest inventories. *ISPRS Journal of Photogrammetry and Remote Sensing* 115:63–77

[19] Oveland I, Hauglin M, Giannetti F, Schipper Kjørsvik N, Gobakken T. 2018. Comparing three different ground based laser scanning methods for tree stem detection. *Remote Sensing* 10:538

[20] Polewski P, Yao W, Cao L, Gao S. 2019. Marker-free coregistration of UAV and backpack LiDAR point clouds in forested areas. *ISPRS Journal of Photogrammetry and Remote Sensing* 147:307–318

[21] Zhou T, Zhao C, Wingren CP, Fei S, Habib A. 2024. Forest feature LiDAR SLAM (F2-LSLAM) for backpack systems. *ISPRS Journal of Photogrammetry and Remote Sensing* 212:96–121

[22] Bauwens S, Bartholomeus H, Calders K, Lejeune P. 2016. Forest inventory with terrestrial LiDAR: a comparison of static and hand-held mobile laser scanning. *Forests* 7:127

[23] Su Y, Guo Q, Jin S, Guan H, Sun X, et al. 2021. The development and evaluation of a backpack LiDAR system for accurate and efficient forest inventory. *IEEE Geoscience and Remote Sensing Letters* 18:1660–1664

[24] Campbell MJ, Dennison PE, Hudak AT, Parham LM, Butler BW. 2018. Quantifying understory vegetation density using small-footprint airborne lidar. *Remote Sensing of Environment* 215:330−342
[25] Cifuentes R, Van der Zande D, Farifteh J, Salas C, Coppin P. 2014. Effects of voxel size and sampling setup on the estimation of forest canopy gap fraction from terrestrial laser scanning data. *Agricultural and Forest Meteorology* 194:230−240
[26] Cabo C, Del Pozo S, Rodríguez-Gonzálvez P, Ordóñez C, González-Aguilera D. 2018. Comparing terrestrial laser scanning (TLS) and wearable laser scanning (WLS) for individual tree modeling at plot level. *Remote Sensing* 10:540
[27] Cheng L, Chen S, Liu X, Xu H, Wu Y, et al. 2018. Registration of laser scanning point clouds: a review. *Sensors* 18:1641
[28] Shao J, Yao W, Wan P, Luo L, Wang P, et al. 2022. Efficient co-registration of UAV and ground LiDAR forest point clouds based on canopy shapes. *International Journal of Applied Earth Observation and Geoinformation* 114:103067
[29] Liu C, Xing Y, Duanmu J, Tian X. 2018. Evaluating different methods for estimating diameter at breast height from terrestrial laser scanning. *Remote Sensing* 10:513
[30] Wang Z, Yin M, Dong J, Zheng H, Ou D, et al. 2022. Multi-view point clouds registration method based on overlap-area features and local distance constraints for the optical measurement of blade profiles. *IEEE/ASME Transactions on Mechatronics* 27:2729−2739
[31] Zhao B, Yue J, Tang Z, Chen X, Fang X, et al. 2023. A novel local feature descriptor and an accurate transformation estimation method for 3-D point cloud registration. *IEEE Transactions on Instrumentation and Measurement* 72:1−15
[32] Inoue A. 2001. Can the relative stem taper curve be estimated theoretically only from tree height and diameter at breast height? *Journal of Forest Planning* 7:89−94
[33] Giannetti F, Puletti N, Quatrini V, Travaglini D, Bottalico F, et al. 2018. Integrating terrestrial and airborne laser scanning for the assessment of single-tree attributes in Mediterranean forest stands. *European Journal of Remote Sensing* 51:795−807
[34] Camarretta N, Harrison PA, Lucieer A, Potts BM, Davidson N, et al. 2021. Handheld laser scanning detects spatiotemporal differences in the development of structural traits among species in restoration plantings. *Remote Sensing* 13:1706
[35] Zhang W, Qi J, Wan P, Wang H, Xie D, et al. 2016. An easy-to-use airborne lidar data filtering method based on cloth simulation. *Remote Sensing* 8:501
[36] Han D, Xu M, Jin Y. 2020. Filtering and accuracy analysis of multi-source heterogeneous point cloud registration data. *Journal of Geomatics Science and Technology* 37:503−508
[37] Zhang W, Zhou F, Wang L, Sun P. 2021. Region growing based on 2-D–3-D mutual projections for visible point cloud segmentation. *IEEE Transactions on Instrumentation and Measurement* 70:5010613
[38] Wang K, Zhou J, Zhang W, Zhang B. 2021. Mobile LiDAR scanning system combined with canopy morphology extracting methods for tree crown parameters evaluation in orchards. *Sensors* 21:339
[39] Xia S, Chen D, Wang R, Li J, Zhang X. 2020. Geometric primitives in LiDAR point clouds: a review. *IEEE Journal of Selected Topics in Applied Earth Observations and Remote Sensing* 13:685−707
[40] Vo AV, Truong-Hong L, Laefer DF, Bertolotto M. 2015. Octree-based region growing for point cloud segmentation. *ISPRS Journal of Photogrammetry and Remote Sensing* 104:88−100
[41] Nurunnabi A, Sadahiro Y, Lindenbergh R, Belton D. 2019. Robust cylinder fitting in laser scanning point cloud data. *Measurement* 138:632−651
[42] McTague JP, Weiskittel A. 2021. Evolution, history, and use of stem taper equations: a review of their development, application, and implementation. *Canadian Journal of Forest Research* 51:210−235
[43] Lee Y, Lee J. 2024. Evaluation of accuracy in estimating diameter at breast height based on the scanning conditions of terrestrial laser scanning and circular fitting algorithm. *Forests* 15:313
[44] Sparks AM, Smith AMS. 2022. Accuracy of a LiDAR-based individual tree detection and attribute measurement algorithm developed to inform forest products supply chain and resource management. *Forests* 13:3
[45] Tian D, Jiang L, Shahzad MK, He P, Wang J, et al. 2022. Climate-sensitive tree height-diameter models for mixed forests in Northeastern China. *Agricultural and Forest Meteorology* 326:109182
[46] Mak NPL, Siu TY, Law YK, Zhang H, Sui S, et al. 2025. Mapping individual tree- and plot-level biomass using handheld mobile laser scanning in complex subtropical secondary and old-growth forests. *Remote Sensing* 17:1354
[47] Ryding J, Williams E, Smith MJ, Eichhorn MP. 2015. Assessing handheld mobile laser scanners for forest surveys. *Remote Sensing* 7:1095−1111